

HETEROCYCLES, Vol. 104, No. 5, 2022, pp. 917 - 924. © 2022 The Japan Institute of Heterocyclic Chemistry  
Received, 6th December, 2021, Accepted, 28th January, 2022, Published online, 4th February, 2022  
DOI: 10.3987/COM-21-14604

## CHARACTERIZATION AND ANTITUMOR ACTIVITY OF FURAZANO[3,4-*g*]PTERIDINE-2,4(1*H*,3*H*)-DIONE

Yoshimasa Makita<sup>1\*</sup> Shin-ichi Kawaguchi,<sup>2</sup> and Shin-ichi Fujiwara<sup>1</sup>

<sup>1</sup> Department of Chemistry, Osaka Dental University, 8-1 Kuzuhahanazono, Hirakata, Osaka 573-1121, Japan; Email: makita@cc.osaka-dent.ac.jp

<sup>2</sup> Center for Education and Research in Agricultural Innovation, Faculty of Agriculture, Saga University, Saga 847-0021.

**Abstract** – Alloxazine derivatives exhibit a wide variety of properties imparted by their tautomerization to isoalloxazine and the presence of similar H-bonding to uracil. Herein, we characterized the structure and properties of furazano[3,4-*g*]pteridine-2,4(1*H*,3*H*)-dione (**1**) by X-ray crystal structure analysis and evaluated its antitumor activity. The IC<sub>50</sub> value of **1** was 172 μM, as determined using HeLa cells.

### INTRODUCTION

The condensed form of the pyrimido[4,5-*b*]quinoxaline ring system is called alloxazine (Figure 1(a)); it exhibits a wide variety of properties because it tautomerizes to isoalloxazine via intramolecular proton transfer. Alloxazine and its derivatives have been used as organocatalysts,<sup>1</sup> ligands of metal complexes,<sup>2</sup> and adenosine receptor antagonists.<sup>3</sup> Alloxazine binds selectively to adenine because H-bonding structure of alloxazine is similar to that of uracil (Figure 1(b)).<sup>4</sup> Moreover, owing to its antitumor activity, alloxazine has attracted much attention in recent years. Alloxazine derivatives reportedly inhibit protein tyrosine kinases that are involved in various forms of cancer.<sup>5</sup> Alloxazine derivatives of 7,8-dimethylalloxazine (lumichrome) showed the inhibition of the growth of lung cancer cells by suppressing the growth and mediating apoptosis of cancer stem cells.<sup>6</sup>

Despite these properties of alloxazine derivatives, their structures and properties have not been extensively studied, unlike those of lumichrome, which is a tautomer of riboflavin. There are only a limited number of reported examples of compounds in which the leftmost ring of alloxazine is a five-membered ring.<sup>7</sup> We focused on the furazano ring, a small five-membered ring without a hydrogen group. By changing the aromatic ring moiety of alloxazine to furazano ring, the alloxazine becomes smaller than those reported so far, and its structure expects closer to uracil. We were curious to see the

properties and the antitumor properties. In this study, we characterized the structure and properties of furazano[3,4-*g*]pteridine-2,4(1*H*,3*H*)-dione (**1**; Figure 1(c)) and evaluated its antitumor activity.

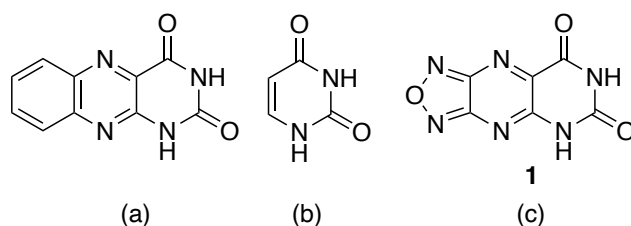
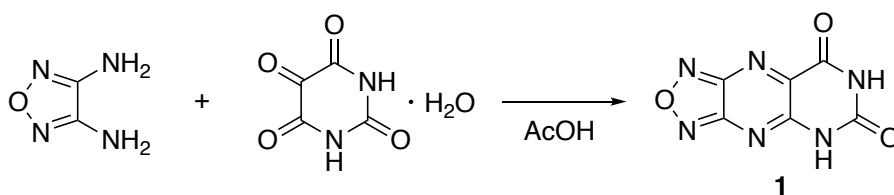


Figure 1. (a) alloxazine, (b) uracil, and (c) furazano[3,4-*g*]pteridine-2,4(1*H*,3*H*)-dione **1**

## RESULTS AND DISCUSSION

The condensation of 3,4-diaminofurazan with alloxan monohydrate in acetic acid at 60 °C for 12 h afforded **1** as a yellow solid in Scheme 1. Compound **1** was purified using silica gel column chromatography. Compound **1** was soluble in dimethyl sulfoxide, sparingly soluble in methanol and acetone, and insoluble in dichloromethane and ethyl acetate. Compound **1** was stable under ambient air and temperature conditions. The mass of **1** was also confirmed through ESI-TOF-MS.



Scheme 1. The condensation reaction of 3,4-diaminofurazan with alloxan monohydrate

The absorption and emission spectra of **1** were measured in Figure 2. The absorption bands of **1** were centered at 285 and 364 nm in water and at 284 and 357 nm in 1,4-dioxane. The emission band of **1** was centered at 428 nm in water and at 417 nm in 1,4-dioxane. The emission intensity of **1** was lower in water than that in 1,4-dioxane. It was reported that H<sub>2</sub>O quenches the fluorescence of several organic chromophores containing proton donor group.<sup>8</sup> The quenching of **1** was probably due to the NH hydrogen in acting as a proton-donating group. The absorption spectra exhibited minimal sensitivity to solvent polarity, whereas the emission intensities were more susceptible to environmental changes.

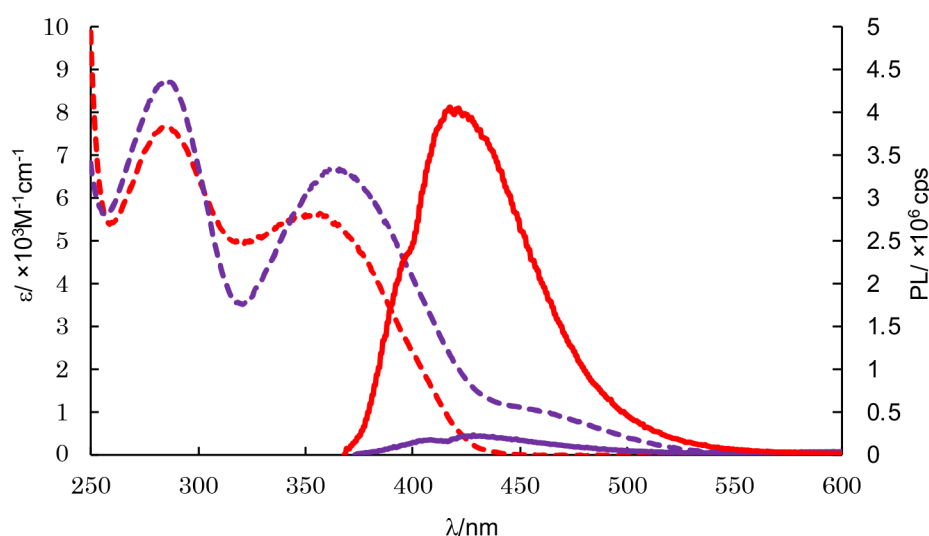
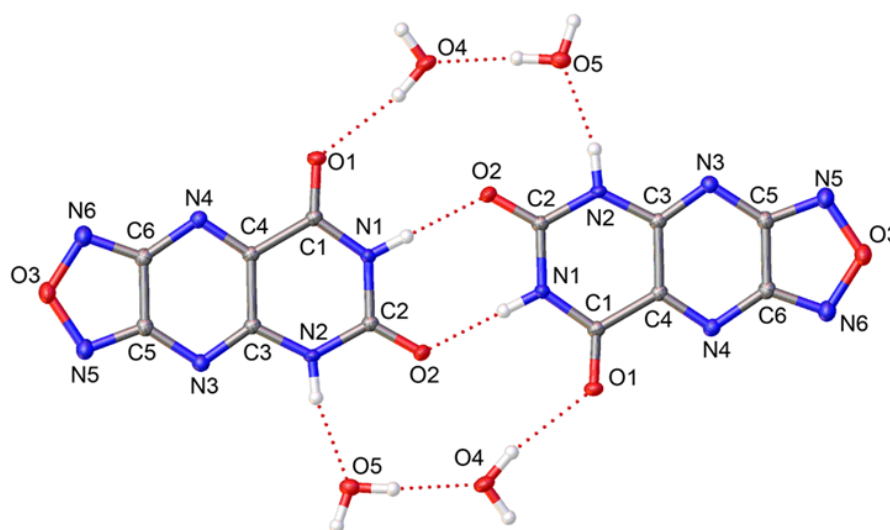


Figure 2. Absorption (dashed lines) and emission (solid lines) spectra of **1** (54  $\mu\text{M}$ ) in 1,4-dioxane (red) and water (blue)

The crystals of **1** were obtained by dissolving and retaining the compound in methanol and dichloromethane at room temperature. The structure is shown in Figure 3 and Table 1. Compound **1** crystallized in the monoclinic space group  $P2_1/c$ . The C(2)–C(3)–C(5) angle was measured as [a C(2)–C(3)–C(5) = 179.1°], and the N(1)–C(4)–C(6) angle was measured as [a N(1)–C(4)–C(6) = 177.6°] (Table S1). These results indicate that **1** has a planar structure. The intermolecular N(1)–O(2) distance was measured as [d N(1)–O(2) = 2.781 Å], indicating that hydrogen bonding interactions were observed between the two molecules of **1**. The intermolecular N(2)–O(5) distance was measured as [d N(2)–O(5) = 2.814 Å], indicating that hydrogen bonding interactions were observed between the N(2) of **1** and O(5) of H<sub>2</sub>O. These results clearly indicate that the protons are bonded to N(1) and N(2), and not to N(4). Therefore, the structure of **1** was confirmed to be similar to that of alloxazine rather than isoalloxazine. The N–O bond lengths of the furazan were measured as [d N(6)–O(3) = 1.374 Å] and [d N(5)–O(3) = 1.396 Å]. The measured C–N bonds of the pyrazine ring were slightly longer ([d N(3)–C(5) = 1.368 Å] [d(N(4)–C(6) = 1.372 Å)] than those of [d(N(3)–C(3) = 1.302 Å] and [d(N(4)–C(4) = 1.297 Å].

Figure 3. X-Ray crystal structure of **1**Table 1. Single crystal X-ray analysis data of **1**

Deposition number	2087351
Empirical formula	C <sub>6</sub> H <sub>6</sub> N <sub>6</sub> O <sub>5</sub>
Molecular formula	C <sub>6</sub> H <sub>2</sub> N <sub>6</sub> O <sub>3</sub> , 2(H <sub>2</sub> O)
Formula weight	242.17
Temperature	100.0 K
Wavelength	0.71073 Å
Crystal system	Monoclinic
Space group	<i>P</i> 2 <sub>1</sub> / <i>c</i>
Unit cell dimensions	<i>a</i> = 5.4131(2) Å, $\alpha$ = 90° <i>b</i> = 26.9646(12) Å, $\beta$ = 113.4160(10)° <i>c</i> = 6.7015(3) Å, $\gamma$ = 90°.
Crystal size	0.3 x 0.24 x 0.18 mm <sup>3</sup>
Crystal color, habit	light yellow irregular
Theta range for data collection	3.398 to 27.109°.
Index ranges	-6 ≤ <i>h</i> ≤ 6, -17 ≤ <i>k</i> ≤ 34, -8 ≤ <i>l</i> ≤ 8
Reflections collected	10107
Independent reflections	1969 [R(int) = 0.0272]
Completeness to theta = 25.242°	99.8%
Absorption correction	Semi-empirical from equivalents
Max. and min. transmission	0.4912 and 0.45
Refinement method	Full-matrix least-squares on F <sup>2</sup>

HeLa cells were used to investigate the antitumor activity of **1**. The viabilities of the HeLa cells were shown in Figure 4. 5-Fluorouracil,<sup>9</sup> cisplatin,<sup>10</sup> alloxazine, and lumichrome were used as controls. The IC<sub>50</sub> values and cell viabilities at 200 μM were summarized in Table 2. Cisplatin showed strong antitumor activity even at low concentrations in HeLa cells. The cell viability was 0% and the IC<sub>50</sub> value was 16 μM (entry 1). On the contrary, 5-fluorouracil demonstrated no antitumor activity in our condition. The cell

viability was 82% at 200  $\mu\text{M}$  and the  $\text{IC}_{50}$  value  $>200$   $\mu\text{M}$  (entry 2). Alloxazine also showed no antitumor activity (entry 3). Lumichrome did not show antitumor activity up to 100  $\mu\text{M}$ , however, the cell viability was a significant decrease to 15% at 200  $\mu\text{M}$  and the  $\text{IC}_{50}$  was estimated to be 160  $\mu\text{M}$  (entry 4). Chantarawong *et al.* reported that lumichrome exhibited the same level of antitumor activity as that of cisplatin in other cancer cells.<sup>6</sup> Therefore, we concluded that lumichrome also exhibited antitumor activity in HeLa cells. By contrast, **1** also significantly decrease the cell viability to 41% at 200  $\mu\text{M}$  (entry 5). The  $\text{IC}_{50}$  value of **1** estimated 172  $\mu\text{M}$ . Although the mechanism by which **1** exhibited antitumor activity needs to be investigated in detail, these results indicate that **1** demonstrates antitumor activity.

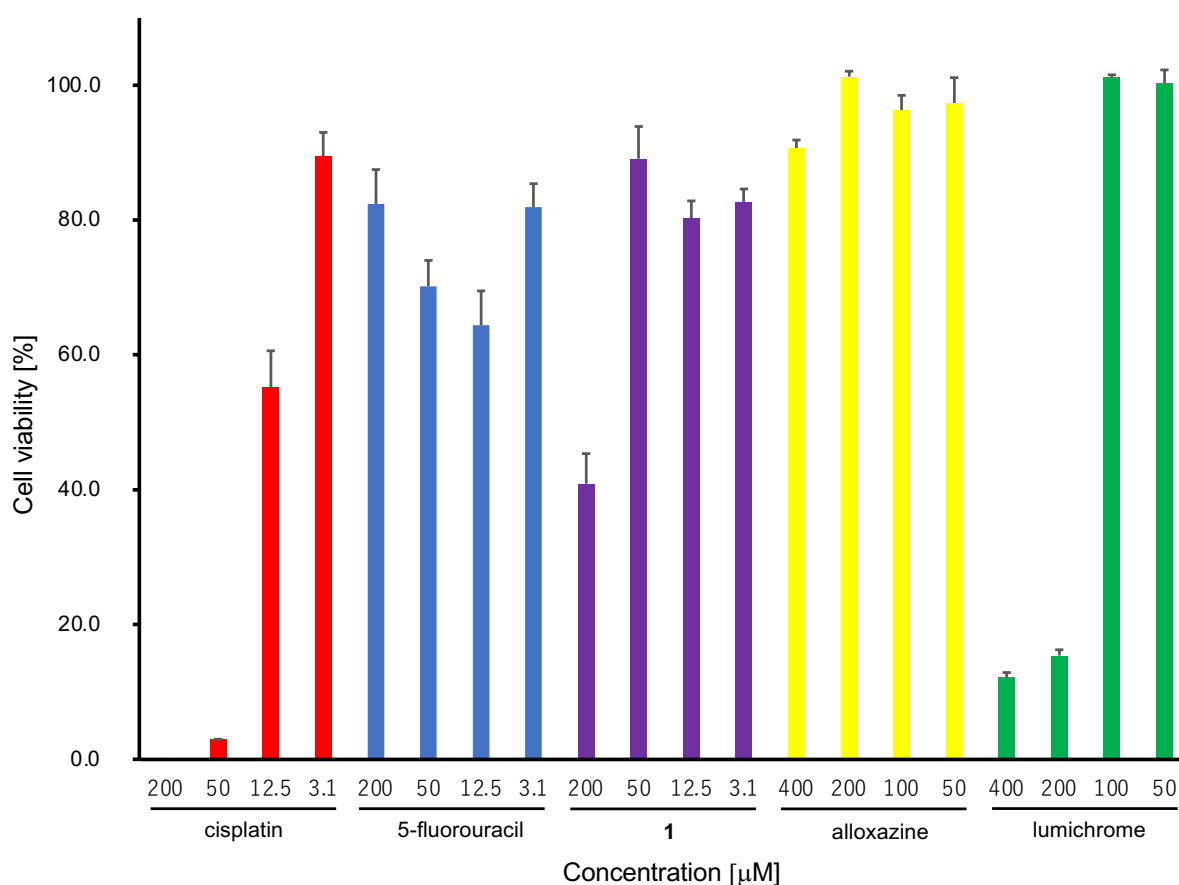


Figure 4. Comparison of cell viabilities of cisplatin, 5-fluorouracil, **1**, alloxazine, and lumichrome in HeLa cells

Table 2. Antitumor activities of compound **1**

Entry	Compound	Cell viability $\pm$ SD at 200 $\mu\text{M}$ [%]	$\text{IC}_{50} \pm$ SD [ $\mu\text{M}$ ]
1	cisplatin	$0 \pm 0.3$	$16 \pm 1.9$
2	5-fluorouracil	$82 \pm 5.1$	$>200$
3	alloxazine	$101 \pm 0.8$	$>200$
4	lumichrome	$15 \pm 0.9$	$160 \pm 4.0$
5	<b>1</b>	$41 \pm 4.5$	$172 \pm 8.0$

Furazano[3,4-*g*]pteridine-2,4(1*H*,3*H*)-dione **1** was characterized as an alloxazine structure through X-ray crystal structure analysis. The antitumor activity of **1** was evaluated in HeLa cells. Compound **1** exhibited antitumor activity.

## EXPERIMENTAL

### Reagents and Instruments

3,4-Diaminofurazan (97%), alloxazine, and alloxan monohydrate were purchased from Sigma-Aldrich. Cisplatin, 5-fluorouracil, and lumichrome were purchased from TCI. Solvents were obtained from Sigma-Aldrich and Fisher Scientific, and dried using standard techniques. Spectroscopy-grade 1,4-dioxane were obtained from Sigma-Aldrich, and aqueous solutions were prepared with deionized water. NMR solvents were purchased from Cambridge Isotope Laboratories (Andover, MA, USA). Column chromatography was performed using a Teledyne ISCO Combiflash Rf. NMR spectra were measured using a JEOL 500 MHz spectrometer. Mass spectra were obtained on an Agilent 6230 HR-ESI-TOF MS.

Single-crystal X-ray diffraction analysis was performed on a Bruker X8 Apex II CCD diffractometer equipped with Mo K $\alpha$  radiation ( $\lambda = 0.71073$ ). A  $0.300 \times 0.240 \times 0.070$  mm light yellow crystal was mounted on a Cryoloop with Paratone oil. The data were collected in a nitrogen gas stream at 100(2) K using  $\phi$  and  $\omega$  scans. The crystal-to-detector distance was 40 mm using a variable exposure time of 2 s and a scan width of  $0.7^\circ$ . Data collection was 99.8% complete to  $25.242^\circ$  in  $\theta$ . A total of 10107 reflections were collected covering the indices  $-6 \leq h \leq 6$ ,  $-17 \leq k < 34$ ,  $-8 \leq l \leq 8$ . The symmetry-independent reflections (1969) exhibited an  $R_{int}$  of 0.0272. Indexing and unit cell refinement indicated a primitive monoclinic lattice. The space group is  $P2_1/c$ .

Absorption spectra were measured using a Shimadzu UV-2450 spectrophotometer with a slit set at 1 nm and a resolution of 0.5 nm. All spectra were corrected with a blank. Emission spectra were obtained using a Horiba Fluoromax-4 equipped with a cuvette holder with a stirring system using both the excitation and emission slits at 3 nm, a resolution of 1 nm, and an integration time of 0.1 s. All spectra were corrected for the blank. The temperature was maintained at  $25.00 \pm 0.10$  °C.

Cell Culture and Antitumor Activity Measurement: The cervical cancer cell line HeLa was purchased from the JCRB Cell Bank (Osaka, Japan). HeLa cells were cultured in Dulbecco's Modified Eagle Medium (DMEM) (Wako, Osaka, Japan) containing 10% fetal bovine serum (Corning, Woodland, CA, USA) and antibiotics (100 U/mL penicillin and 100  $\mu$ g/mL streptomycin) in a humidified atmosphere

with 5% CO<sub>2</sub> at 37 °C. The viability of the HeLa cells was measured by the Cell Counting Kit-8 (CCK-8; Dojindo, Kumamoto, Japan). The cells were seeded in 96-well microplates with 1600 cells each. After 24 h of incubation, the cells were stimulated with each compound and incubated for an additional 24 h. Then, 10 µL of CCK-8 solution was added to each well of the plate. After 2 h of incubation at 37 °C, the absorbance of each well (at 450 nm) was measured using a microplate reader (AS ONE MPR-A100). Wells with culture media were used as negative controls. Wells with 0.1% DMSO were used as positive controls. Measurements were performed with n = 3 per sample, and the cells were stimulated at concentrations of 400, 200, 50, 12.5, and 3.1 µM. Moreover, 50% absorbance (A50%) was calculated from the absorbance (A0%) of the negative control and the absorbance (A100%) of the positive control. The relation between cell viability and concentration was plotted and IC<sub>50</sub> was calculated for each compound.

**Furazano[3,4-g]pteridine-2,4(1H,3H)-dione (1)** To a 50 mL round bottomed flask, 3,4-diaminofurazan (300 mg, 3.00 mmol), alloxan monohydrate (480 mg, 3.00 mmol), and acetic acid (30.0 mL) were added under Ar at room temperature. The suspension was then heated at 60 °C for 12 h and the resulting mixture was filtered and evaporated.

The residue was purified by silica gel column chromatography with a gradient of 0%–10% MeOH in DCM (Rf: 0.2 in 10% MeOH in DCM) to give **1** (225 mg, 37%) as a yellow solid.

<sup>1</sup>H NMR (500 MHz, DMSO-*d*<sub>6</sub>): δ 12.25 (br, 1H), 12.63 (br, 1H) ppm, <sup>13</sup>C NMR (100 MHz, DMSO-*d*<sub>6</sub>): δ 144.6, 150.1, 151.5, 152.4, 158.8 ppm.; HR-ESI-MS: *m/z* Calcd for C<sub>6</sub>H<sub>6</sub>N<sub>6</sub>O<sub>3</sub> [M-H]<sup>-</sup> 205.0116, found 205.0117. Mp 113.8–114.2 °C. IR (KBr) 3229, 1730 cm<sup>-1</sup>.

## ACKNOWLEDGEMENTS

Compound **1** was synthesized and characterized at Prof. Ytzhak Tor's laboratory in University of California, San Diego (UCSD). We appreciate Prof. Ytzhak Tor for his dedicated support. We thank Dr. Milan Gembicky for measuring X-ray crystal structure analysis in UCSD.

## REFERENCES

- (a) V. Mojr, M. Buděšínský, R. Cibulka, and T. Kraus, *Org. Biomol. Chem.*, 2011, **9**, 7318; (b) S. Chen and F. W. Foss, Jr., *Org. Lett.*, 2012, **19**, 5150; (c) H. Guo, H. Xia, X. Ma, K. Chen, C. Dang, J. Zhao, and B. Dick, *ACS Omega*, 2020, **5**, 10586.
- W. Kaim, B. Schwederski, O. Heilmann, and F. M. Hornung, *Coord. Chem. Rev.*, 1999, **182**, 323.
- (a) L. E. Brackett and J. W. Daly, *Biochem. Pharmacol.*, 1994, **47**, 801; (b) H. G. Lee, W. M. Kim, J. I. Choi, and M. H. Yoon, *Neurosci. Lett.*, 2010, **480**, 182.
- (a) B. Rajendar, S. Nishizawa, and N. Teramae, *Org. Biomol. Chem.*, 2008, **6**, 670; (b) B. Rajendar,

- A. Rajendran, Z. Ye, E. Kanai, Y. Sato, S. Nishizawa, M. Sikorski, and N. Teramae, *Org. Biomol. Chem.*, 2010, **8**, 4949.
5. (a) H. I. Ali, K. Tomita, E. Akaho, H. Kambara, S. Miura, H. Hayakawa, N. Ashida, Y. Kawashima, T. Yamagishi, H. Ikeya, F. Yoneda, and T. Nagamatsu, *Bioorg. Med. Chem.*, 2007, **15**, 242; (b) H. I. Ali, K. Tomita, E. Akaho, M. Kunishima, Y. Kawashima, T. Yamagishi, and T. Nagamatsu, *Eur. J. Med. Chem.*, 2008, **43**, 1376; (c) W. H. Malki, A. M. Gouda, H. E. A. Ali, R. Al-Rousan, D. Samaha, A. N. Abdalla, J. Bustamante, Z. Y. A. Elmageed, and H. I. Ali, *Eur. J. Med. Chem.*, 2018, **152**, 31; (d) S. Mahmoud, D. Samaha, M. S. Mohamed, N. A. A. Taleb, M. A. Elsayy, T. Nagamatsu, and H. I. Ali, *Molecules*, 2020, **25**, 2518.
6. W. Chantarawong, N. Kuncharoen, S. Tanasupawat, and P. Chanvorachote, *Nutr. Cancer*, 2019, **71**, 1390.
7. (a) J. Quiroga, N. E. Sánchez, P. Acosta, B. Insuasty, and R. Abonia, *Tetrahedron Lett.*, 2012, **53**, 3181; (b) J. Richtar, P. Heinrichova, D. H. Apaydin, V. Schmiedova, C. Yumusak, A. Kovalenko, M. Weiter, N. S. Sariciftci, and J. Krajcovic, *Molecules*, 2018, **23**, 2271; (c) M. Isbera, B. Bognar, G. Gulyas-Fekete, K. Kish, and T. Kalai, *Synthesis*, 2019, **51**, 4463.
8. L. Stryer, *J. Am. Chem. Soc.*, 1966, **88**, 5708.
9. D. B. Longley, D. P. Harkin, and P. G. Johnston, *Nat. Rev. Cancer*, 2003, **3**, 330.
10. L. Kelland, *Nat. Rev. Cancer*, 2007, **7**, 573.